Accelerated Intramolecular Charge Transfer in Tetracyanobutadiene and Tetracyanoquinodimethane Incorporated Asymmetric Triphenylamine-Quinoxaline Push-Pull Conjugates

Youngwoo Jang, Bijesh Sekaran, Prabal P Singh, Rajneesh Misra,* and Francis D'Souza *

Abstract: Excited state properties of an asymmetric triphenylamine-quinoxaline push-pull system wherein triphenylamine, and quinoxaline take up the roles of electron donor and acceptor, respectively, are initially investigated. Further, in order to improve the push-pull effect, powerful electron acceptors, viz., 1,1,4,4-tetracyanobutadiene (TCBD) and cyclohexa-2,5-diene-1,4-diylidene-expanded tetracyanobutadiene (also known tetracyanoquinodimethane, TCNQ) have been introduced into the triphenylamine-quinoxaline molecular framework using catalyst-free [2+2] cycloaddition-retroelectrocyclization reaction. The presence of these electron acceptors caused strong ground-state polarization extending the absorption well into the near-IR region accompanied by strong fluorescence quenching due to intramolecular charge transfer. Systematic studies were performed using a suite of spectral, electrochemical, computational, and pump-probe spectroscopic techniques to unravel the intramolecular charge transfer mechanism and to probe the role of TCBD and TCNQ in promoting excited-state charge transfer and separation events. Faster charge transfer in TCNQderived compared to that in TCBD-derived push-pull systems has been witnessed in polar benzonitrile.

Introduction

The significance of light-driven electron transfer reactions in chemical, physical, and biological processes has become of paramount importance during the last two to three decades.¹⁻⁷ In covalently linked donor-acceptor (D-A) systems, electron transfer reactions are generally studied in polar solvents where the charge-separated states are stabilized by strong solvation. In nonpolar solvents, only partial charge transfer occurs especially when the driving force is small. The introduction of a stronger secondary electron acceptor or a stronger secondary electron donor could help in moving the charge transfer and separation processes forward by improving the overall driving force.¹⁻⁷

Recently, the photophysical studies of aza-derivatives of 1,2-diarayl-ethylenes, such as quinoxaline have received considerable attention as the n,π^* states introduced by nitrogen atoms influence their properties.^{8,9} A few examples of donor-acceptor systems derived from quinoxaline are also known in the literature,¹⁰⁻¹⁶ and such systems have been found useful not only to study electron transfer but also to seek aggregation-induced fluorescence and nonlinear optical applications.¹⁴⁻²¹

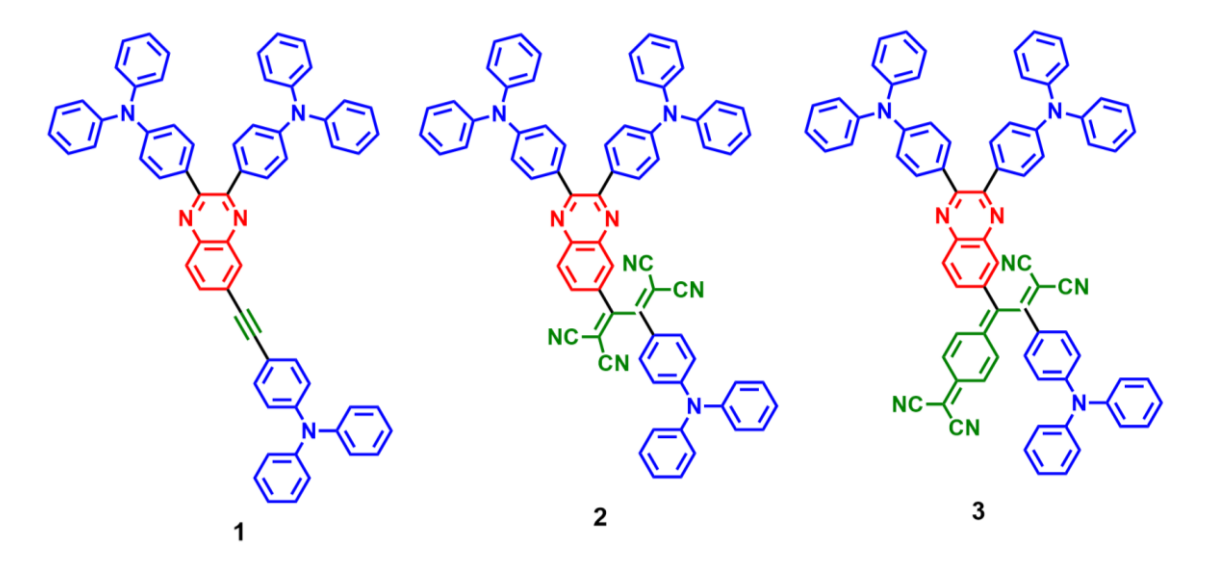


Fig. 1. Structure of the investigated quinoxaline-derived D-A, D-A'-A (D=triphenylamine, A=quinoxaline, and A'=TCBD or TCNQ) type push-pull systems.

In the present study, we report an asymmetric triphenylamine-quinoxaline push-pull system, **1** wherein triphenylamine and quinoxaline take up the roles of electron donor and acceptor, respectively (see Fig. 1 for structures). Further, in order to improve the push-pull effect, powerful secondary electron acceptors, viz., 1,1,4,4-tetracyanobutadiene (TCBD) and

cyclohexa-2,5-diene-1,4-diylidene-expanded tetracyanobutadiene (TCNQ)²²⁻⁴² (compounds **2** and **3**) are introduced using catalyst-free [2+2] cycloaddition-retroelectrocyclization reaction according to the general procedure reported by Diederich⁴³ for this class of compounds. The presence of the secondary electron acceptors caused strong ground-state polarization extending the absorption well into the near-IR region accompanied by strong fluorescence quenching due to intramolecular charge transfer. Systematic studies are performed using a suite of physicochemical techniques to unravel the intramolecular charge transfer mechanism and the role of TCBD and TCNQ in promoting excited-state charge transfer and separation processes, as summarized below.

Experimental Section

General methods

The UV-visible spectral measurements were carried out with a Shimadzu Model 2550 double monochromator UV-visible spectrophotometer. The fluorescence emission was monitored by using a Horiba Yvon Nanolog coupled with time-correlated single photon counting with nanoLED excitation sources. A right-angle detection method was used.

Differential pulse and cyclic voltammograms were recorded on an EG&G 263A electrochemical analyzer using a three electrodes system. A platinum button electrode was used as the working electrode. A platinum wire served as the counter electrode and an Ag/AgCl electrode was used as the reference electrode. Ferrocene/ferrocenium redox couple was used as an internal standard. All the solutions were purged prior to electrochemical and spectral measurements using argon gas.

Femtosecond transient absorption spectroscopy experiments were performed using an ultrafast femtosecond laser source (Libra) by Coherent incorporating a diode-pumped, modelocked Ti:sapphire laser (Vitesse) and a diode-pumped intracavity doubled Nd:YLF laser (Evolution) to generate a compressed laser output of 1.45 W. For optical detection, a Helios transient absorption spectrometer coupled with a femtosecond harmonics generator, both provided by Ultrafast Systems LLC, was used. The sources for the pump and probe pulses were derived from the fundamental output of Libra (Compressed output 1.45 W, pulse width 100 fs) at a repetition rate of 1 kHz; 95% of the fundamental output of the laser was introduced into a TOPAS-Prime-OPA system with a 290–2600 nm tuning range from Altos Photonics Inc., (Bozeman, MT), while the rest of the output was used for generation of a white light continuum.

Kinetic traces at appropriate wavelengths were assembled from the time-resolved spectral data. Data analysis was performed using Surface Xplorer software supplied by Ultrafast Systems. All measurements were conducted in degassed solutions at 298 K. The estimated error in the reported rate constants is $\pm 10\%$.

Results and Discussion

Synthesis of compounds **1-3** is reported by us earlier.⁴⁴ For triphenylamine-linked quinoxaline, **1**, a multi-step synthetic procedure involving, Pd-catalyzed Sonogashira cross-coupling was employed. Compounds **2** and **3** were synthesized by the [2+2] cycloaddition–retroelectrocyclic ring-opening reaction. The compounds were purified by column chromatography and fully characterized by ¹H and ¹³C NMR and HRMS techniques before physico-chemical studies.⁴⁴

The effect of introducing TCBD and TCNQ into the D-A system, 1 in benzonitrile is shown in Fig. 2a. The peak maximum of 1 was located at 440 nm. In the case of 2, this peak experienced a red-shift and considerable broadness (likely overlap of two peaks) and appeared at 467 nm. For 3, this effect was even more drastic, two peaks at 463 and 658 nm were observed. Changing the solvent to nonpolar toluene revealed notable changes (see Fig. S1a in supporting information, SI). While the peak maxima for 1 appeared at 438 nm, that of 2 was split and appeared at 445 and 497 nm. Peaks of 3 were located at 464 and 618 nm. For both 2 and 3, the high-energy peak has been attributed to regular π - π * transition due to its spectral similarity to 1, while the new low-energy peak has been ascribed to the transition involving Pristine quinoxaline (phenyl substituents instead of charge transfer absorption. triphenylamine) is known to reveal absorption in <400 nm. 45 Considerable red shift of the second peak in polar solvent confirms such an assignment (a 30 nm red shift in the case of 2, and a 40 nm red shift in the case of 3 between toluene and benzonitrile). Such a trend was also observed in the fluorescence spectral studies (Fig. 2b and S1b). The fluorescence maximum of 1 in toluene was located at 497 nm (Fig. S1b and c) while in benzonitrile, it was located at 572 nm (Fig. 2b). As expected for polar compounds, an increase in spectral red-shift with an increase in solvent polarity was observed, (see Figure S1c). Lifetime measured for 1 using time-correlated single-photon counting was found to be 5.92 ns in benzonitrile. Interestingly, in the case of both 2 and 3, fluorescence quenching over 98% was witnessed in both solvents (see Figs. 2b and S1b). Weak emission of 2 was located at 578 nm while that of 3 was located at 579 nm when excited at 463 nm. Excitation of 2 at 497 nm and 3 at 658 nm revealed no

emission either in benzonitrile or toluene corresponding to charge transfer emission. It is likely that the charge transfer is too weak and beyond the detection limit of our instrumental setup. Using the absorption and fluorescence spectral data, the energy of excited states, $E_{0,0}$ were subsequently estimated and are listed in Table 1.

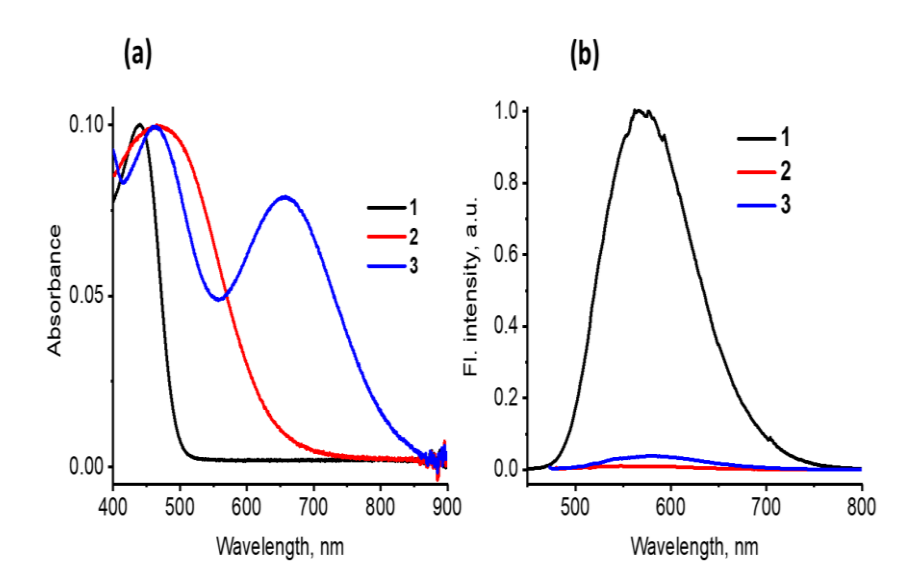


Fig. 2. (a) Absorption and (b) fluorescence spectra of indicated compounds in benzonitrile. Compound 1 was excited at 440 nm, 2 was excited at 425, and 3 was excited at 463 nm.

Table 1. Energies of Singlet Excited States, Charge Transfer States from Computational Studies, Free-energy for Charge Separation and Recombination in Benzonitrile and Toluene.^a

Compound	Solvent	$E_{\theta,\theta}{}^b$	E _{CT} , eV ^c	$\Delta G_{\rm sol}$, eV	- $\Delta G_{\rm CS}$, eV	$-\Delta G_{\rm CR}$, eV
1	PhCN	2.49	2.92	-0.070	0.16	2.52
	Toluene	2.66		1.017	-0.93	3.61
2	PhCN	2.24	2.01	-0.058	0.68	1.71
	Toluene	2.52		0.535	-0.25	2.30
3	PhCN	2.19	1.60	-0.067	1.12	1.09
	Toluene	2.46		0.595	-0.04	1.76

^a-estimated error < 5% for energy values.

^b-from 0,0 transitions of absorption and fluorescence peaks corresponding to the π - π * transition.

^c-gas-phase HOMO-LUMO energy gap from computational studies

Since the push-pull effects are also dictated by the redox potentials of the donor and acceptor entities, an electrochemical investigation was undertaken to evaluate the redox potentials. Both cyclic (CV) and differential pulse voltammetry (DPV) techniques were used; the former to evaluate the electrochemical reversibility and the latter to determine exact redox potentials. The first reduction of compound 1 was located at -1.95 V vs. Fc/Fc⁺ due to the reduction of the quinoxaline entity. On the anodic side, owing to the presence of multiple triphenylamine entities, connected to the central quinoxaline either directly or via an acetylene bridge, three oxidation waves were observed. Among these, the first oxidation process was located at 0.42 V. On the CV timescale, both oxidation and reduction were found to be quasi-reversible to irreversible (Fig. S2).

In compound 2 having an electron-deficient TCBD entity placed between quinoxaline and triphenylamine utilizing the acetylene functionality, two additional reductions corresponding to the step-wise reduction of TCBD at -0.68 and -1.04 V were observed. Due to the electronic effects induced by the TCBD entity, the quinoxaline reduction was cathodically shifted and appeared at -2.26 V. The oxidation of triphenylamine also experienced a small anodic shift and appeared at 0.45 V. The presence of a much more electron-deficient TCNQ in 3 revealed stepwise reductions of TCNQ at -0.32 and -0.54 V. The second reduction process revealed splitting perhaps due to the different structural arrangement of TCNQ- in 3. Quinoxaline reduction was located at -1.96 V while triphenylamine oxidation was located at 0.44 V.

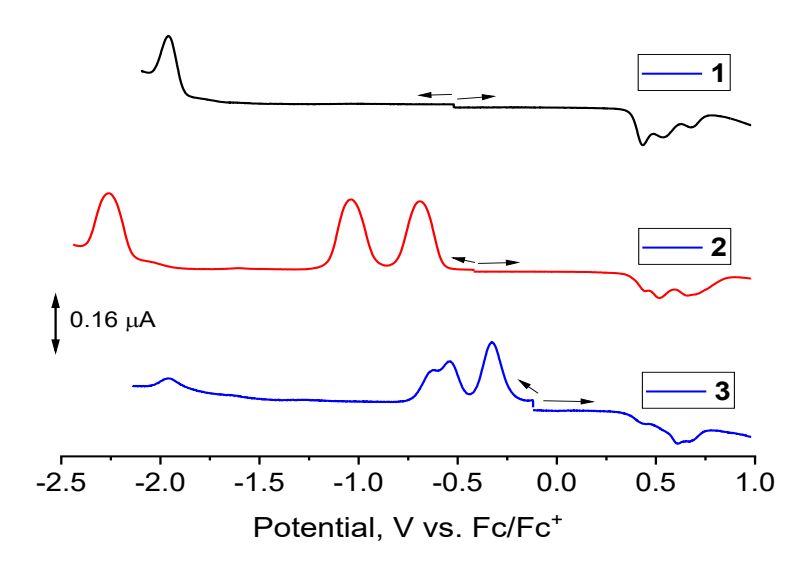


Fig. 3. DPVs of investigated asymmetric quinoxaline compounds with ferrocene as an internal standard in benzonitrile in the presence of 0.1 M tetrabutylammonium perchlorate.

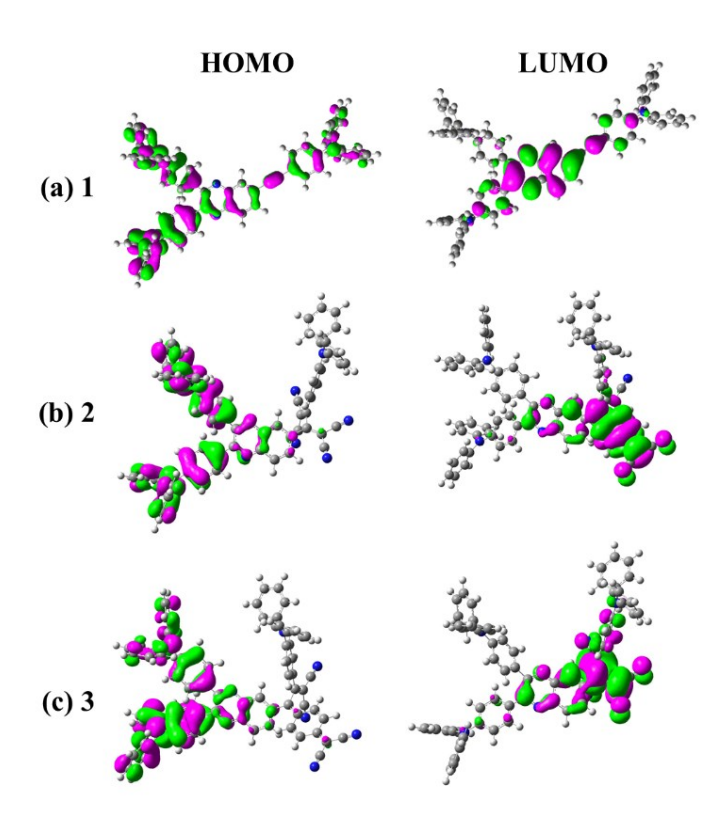


Fig. 4. Frontier HOMO and LUMO of the indicated compounds on B3LYP/6-31G* optimized structures.

Next, the push-pull systems were geometry optimized at the B3LYP/6-31G* level. 46 The optimized structures are shown in Fig. S3 while the frontier HOMO and LUMO are shown in Fig. 4. In the optimized structures, no steric constraints between the adjacent triphenylamine entities directly connected to the quinoxaline or TCBD and TCNQ entities with quinoxaline in 2 and 3 were observed. However, the triphenylamine entity in 2 and 3 was rotated over 64° to accommodate TCBD and TCNQ entities. The HOMO in 1 was found to be spread all over the molecules with relatively higher contributions on the triphenylamine entities directly connected to quinoxaline. Much of the LUMO was localized on the quinoxaline entity. In the case of 2 and 3, the majority of the HOMO was on the triphenylamine entities directly connected to the quinoxaline while the LUMO was on quinoxaline-TCBD in the case of 2 and quinoxaline-TCNQ in the case of 3. These $(TPA)_2^{\delta+}-Qx^{\delta-}-TPA$ of results suggest the formation (TPA=triphenylamine, Qx=quinoxaline) charge transfer state in the case of 1 (transition from TPA centered HOMO to Qx centered LUMO), $(TPA)_2^{\delta+}$ - $(Qx-TCBD)^{\delta-}$ -TPA charge-transfer state in the case of 2 (transition from TPA centered HOMO to Qx-TCBD centered LUMO), and $(TPA)_2^{\delta+}$ - $(Qx-TCNQ)^{\delta-}$ -TPA charge-transfer state in the case of 3 (transition from TPA centered HOMO to Qx-TCNQ centered LUMO). The gas phase HOMO-LUMO energy gap from computational studies (see Table 1) is employed as the energy of the charge transfer state, $E_{\rm CT}$ in the present study. The $E_{\rm CT}$ followed the order: 3 < 2 < 1.

An energy level diagram was subsequently constructed to visualize the excited state events in these push-pull systems. Two solvents, viz., polar benzonitrile and nonpolar toluene were considered. For this construction, singlet excited state energy, $E_{0,0}$ (S₁), E_{CT} from computational studies, and charge separation (ΔG_{CS}) and recombination (ΔG_{CR} , after incorporating solvation energy into the ΔG_{sol} term) were calculated using standard procedure^{47,48} using the earlier discussed redox and computational data (see Table 1). Please note that our repeated attempts to record the phosphorescence of the investigated compounds at liquid nitrogen temperature and various glass-forming solvents did not result in any measurable signal. Hence, the triplet energy level is not depicted in Figure 5.

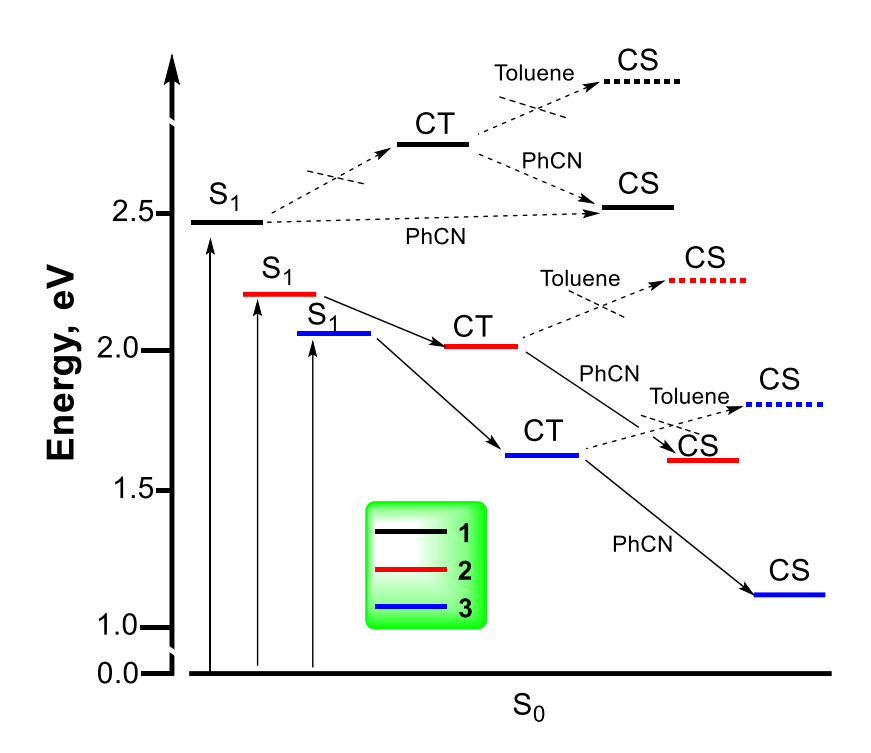


Fig. 5. Energy level diagram depicting energies of the singlet excited (S₁), charge transfer (CT), and charge separation (CS) states of **1** (black line), **2** (red line), and **3** (blue line) in benzonitrile (solid lines) and toluene (dashed lines). (Note: CT of **1** = (TPA)₂δ+-Qxδ--TPA; CT of **2** = (TPA)₂δ+-(Qx-TCBD)δ--TPA and CT of **3** = (TPA)₂δ+-(Qx-TCBD)δ--TPA from computational HOMO-LUMO gap. CS of **1** = (TPA)₂·+-Qx·--TPA; CS of **2** = (TPA)₂·+-(Qx-TCBD)·--TPA and CS of **3** = (TPA)₂·+-(Qx-TCBD)·--TPA from free-energy calculations).

As shown in Figure 5, in the case of 1, the energy of the CT state was higher than that of the S₁ state while the energy of the charge-separated state was close to that of the S₁ state in benzonitrile but not in toluene. This indicates a lack of charge transfer in 1 but the possibility of charge separation directly from the S₁ state. This observation also draws support from the strong fluorescence of 1 observed in both benzonitrile and toluene. Interestingly, in the case of 2 and 3, having powerful electron acceptors, the CT state was well below that of the corresponding S₁ state making the CT process thermodynamically feasible. The earlier discussed fluorescence studies where highly quenched S₁ state in both 2 and 3 was witnessed in both polar and nonpolar solvents draw support to this. Interestingly, the CT state in both 2 and 3 was capable of transforming into a CS state in polar benzonitrile due to additional solvent stabilization of the radical ion pair. However, in toluene, only the CT state and no CS state were possible to visualize from this energy diagram due to unfavorable solvation. That is, the energy of the CS state was higher than the corresponding CT state. A CS state directly from the LE state without the intermediate CT state is also possible in cases of 2 and 3 in benzonitrile. However, due to the presence of ground-state CT in these systems, a CT \rightarrow CS route is considered more favorable.

Thin-layer spectroelectrochemical characterization of the oxidized and reduced species of compounds 1-3 in benzonitrile was subsequently performed, as shown in Fig. S4. Potentials 100 mV past the redox peaks shown in Fig. 3 was applied to generate a given oxidized or reduced species. For 1, well-defined peaks in the visible region (742 nm for oxidized and 584 nm for the reduced species) were observed. For 2, a new peak at 740 nm for the oxidized product was obvious while for 3, increased intensity in this spectral range during oxidation was witnessed. This spectral data was subsequently used to arrive at the spectrum of the charge-separated product. For this, the spectrum of the cationic and anionic species was digitally added and subtracted from that of the neutral compound. Such spectrum is shown in the bottom panel of Fig. S4 was subsequently used to characterize the charge-separated product in these compounds.

Femtosecond transient absorption (fs-TA) spectroscopy was subsequently employed to seek evidence of charge transfer and separation as a function of the solvent polarity of the studied compounds. Fig. 6a shows the fs-TA at the indicated delay times of 1 in benzonitrile. The singlet excited state formed within the first 1-2 ps revealed excited state absorption peaks at 488, and 610 nm, and a shoulder-type peak at 667 nm. The decay of these peaks was accompanied by a new peak at 518 nm that maxed out at about 100 ps and

started decaying. The position and shape of this peak overlapped to some extent from that deduced for the charge-separated state from spectroelectrochemical studies (peak maxima were at 584 nm, see magenta dashed line in Fig. 6a) suggesting that the newly developed spectrum could be due to a charge-separated state. Further, nanosecond transient spectral studies were performed to characterize this species, however, within the earliest detection time of our instrumental setup (\sim 20 ns), no spectrum could be observed suggesting its faster relaxation to the ground state. In summary, as suggested by the energy diagram, no charge transfer was possible, however, a direct charge separation from the S₁ state was plausible in benzonitrile.

The fs-TA spectra recorded for 1 in toluene revealed the excited state absorption band at 605 nm (see Figure 6b), however, decay of this peak did not result in any new peaks in the 500 nm region corresponding to the charge-separated state. This is in accordance with the expectation of the energy diagram where no charge separation is toluene either directly from the S₁ state or via the charge transfer state was anticipated.

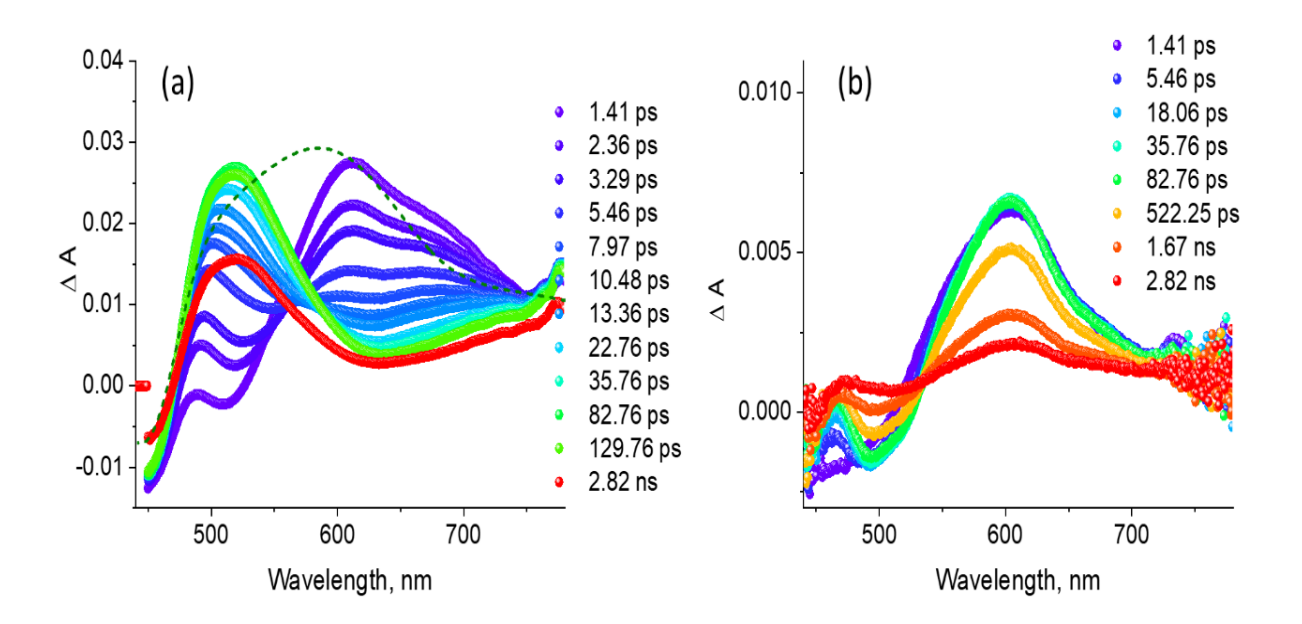


Fig. 6. Fs-TA absorption spectra of 1 ($\lambda_{ex} = 439$ nm) at the indicated delay times in benzonitrile. The dashed magenta line is the spectrum arrived for the charge seperated state from spectroelectrochemical studies.

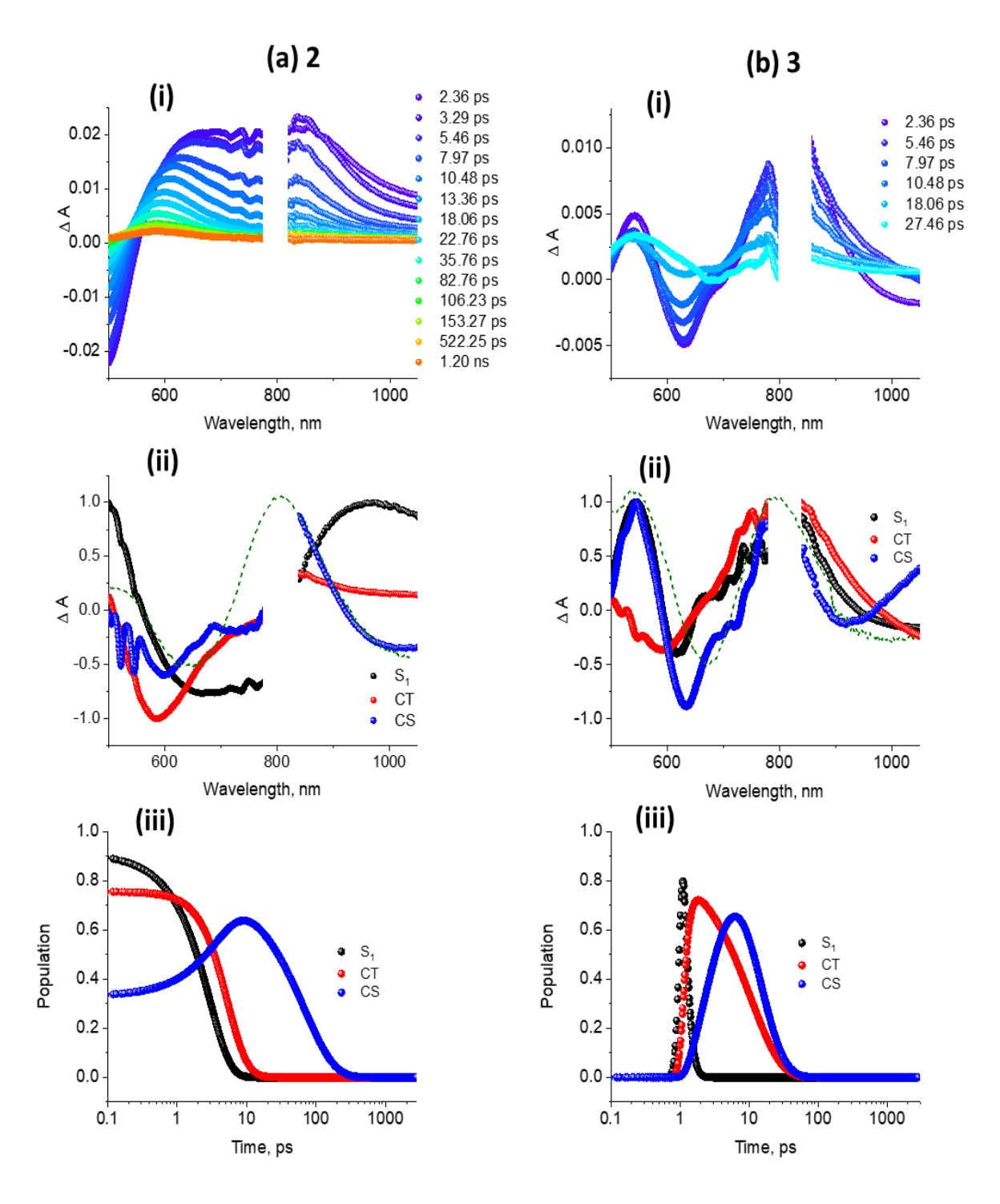


Fig. 7. Fs-TA absorption spectra of (a) 2 ($\lambda_{ex} = 467$ nm) and (b) 3 ($\lambda_{ex} = 463$ nm) at the indicated delay times in benzonitrile. Species-associated spectra (SAS) and population kinetics of species (not normalized) from the global analysis of transient data are given in the bottom panels. The dashed magenta line in the middle panel is the spectrum deduced for the charge-separated state from spectroelectrochemical studies. The break in the 800 nm region is to block the low signal-to-noise signal at the extreme of visible and near-IR detectors.

Table 2. The lifetime of charge transfer and separation as a function of solvent polarity for compounds 2 and 3.^a

Compound	λ_{ex} , nm	solvent	τ _{S1} , ps	τ _{CT} , ps	τ _{CS} , ps
2	467	PhCN	1.4	7.13	67.6
		Toluene	9.80	17.3	
3	463	PhCN	1.18	2.74	10.6
		Toluene	1.56	4.01	

^aestimated error = $\pm 10\%$

Fs-TA spectra of compounds 2 and 3 in benzonitrile are shown in Fig. 7. Unlike for 1, transient features, both growth and decay were rather fast for both compounds and the transient signals were supportive of initial charge transfer and subsequent charge separation processes. Most of the transient signals in the case of 2, within the first 100 ps, and 50 ps in the case of 3, were observed. In the case of 2, recovery of the initial peak at 2.36 ps revealed a short-lived, new peak at 590 nm, likely due to the triplet populated state from the CS state during the process of charge recombination, and relaxed to the ground state within 1 ns. This suggests that the CT state could competitively produce the CS state or populate the triplet excited state. A similar scenario was also observed in the case of 3 where the CT state competatively populating the CS and triplet states could be envisioned. In both cases, the spectrum attributed to the CS state agreed well with that deduced from spectroelectrochemical studies, indicating charge separation in both 2 and 3 in benzonitrile. The data were subjected to global analysis⁴⁹ wherein a three-component fit, representing $S_1 \rightarrow CT \rightarrow CS \rightarrow GS$ was satisfactory (ignoring any hot vibrational and solvent relaxations), as shown in the middle panel of Fig. 7. From the population kinetics (see Fig. 7 bottom panel), the average lifetime of each species arrived and is given in Table 2.

In toluene, the earlier discussed energy diagram suggested the formation of a CT state but not the CS state in the case of both 2 and 3. The transient data were supportive of this rationale wherein the CT state did not provide conclusive evidence of CS formation (see Fig. 8). Consequently, the transient data, shown in Fig. 8, was subjected to a two-component fit representing $S_1 \rightarrow CT \rightarrow GS$. Kinetic values secured from the global analysis are also listed in Table 2. From such data, faster CT and CS processes in 3 compared to 2

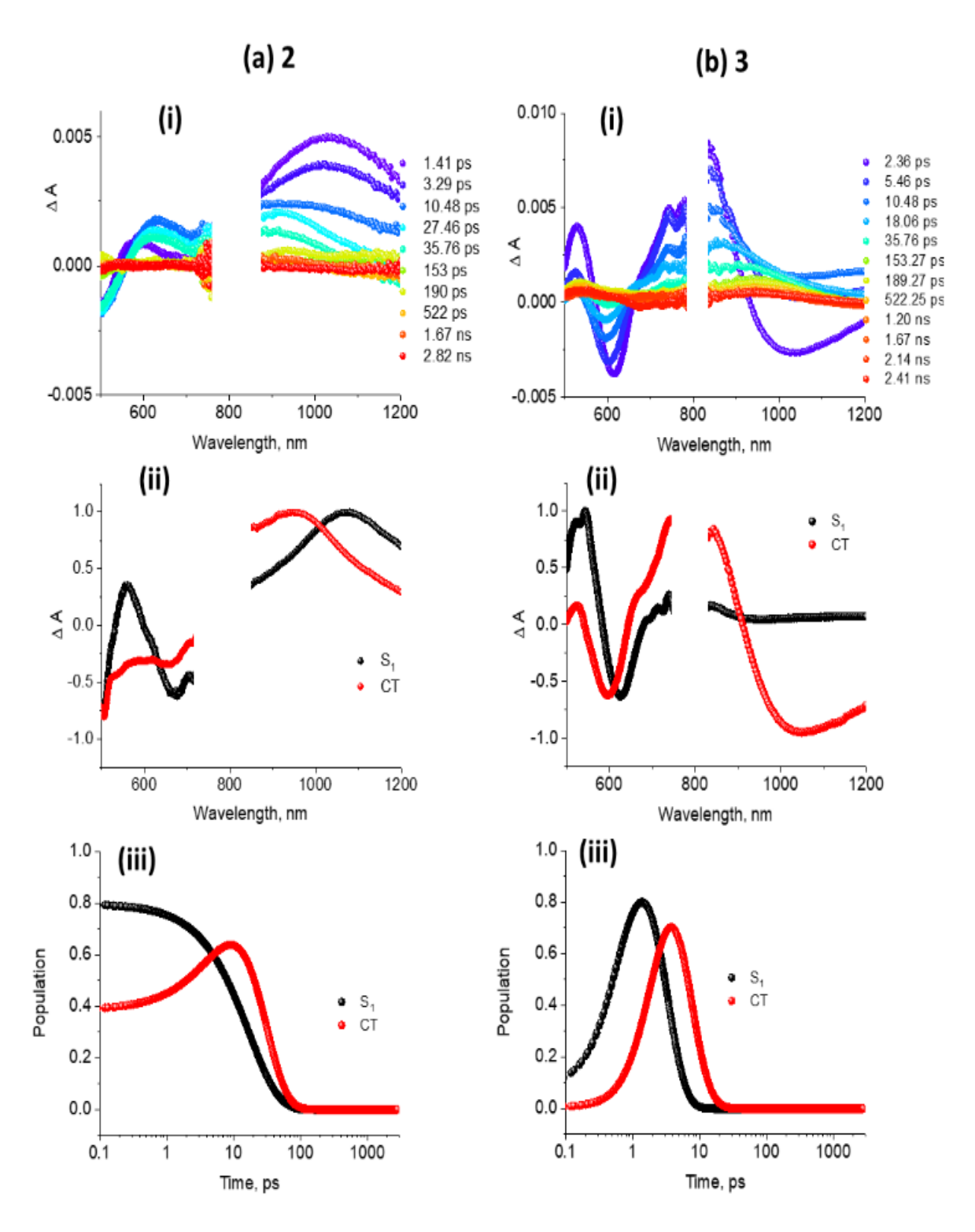


Fig. 8. Fs-TA absorption spectra of (a) 2 (λ_{ex} = 467 nm) and (b) 3 (λ_{ex} = 463 nm) at the indicated delay times in toluene. Species-associated spectra (SAS) and population kinetics (not normalized) of species from the global analysis of transient data are given in the bottom panels. The break in the 800 nm region is to block the low signal-to-noise signal at the extreme of visible and near-IR detectors.

in benzonitrile were obvious and that could be attributed to the relatively higher driving force in the case of 3. The CT formation also followed such a trend in toluene. In both cases, the overall lifetime of the CS state in benzonitrile (67.7 and 10.6 ps) suggests ultrafast charge recombination that could be attributed to the close disposal of the donor-acceptor entities in the studied push-pull systems.

Summary

In conclusion, the introduction of either TCBD or TCNQ into the triphenylamine-quinoxaline structure is shown to cause drastic effects in terms of their optical coverage due to charge transfer and the ability to undergo efficient excited-state events leading to efficient charge transfer. Systematic studies involving electrochemical, spectroelectrochemical, computational, and transient spectroscopic techniques helped in rationalizing the occurrence of photo-events at the picosecond timescale due to their close proximity and a high driving force as depicted in Figure 5 (energy difference between the S₁ and CS states). Further, the formation of charge separated state from the initial charge transfer state was possible to witness in polar benzonitrile but not in nonpolar toluene. Overall, TCNQ-carrying compound 3 revealed a faster occurrence of charge transfer compared to TDBD-carrying compound 2. The persistence of the CS state in benzonitrile also followed such a trend as expected based on their energy considerations.

Acknowledgment

We acknowledge support from the National Science Foundation, USA (2000988 to FD), SERB Project No. (CRG/2022/000023), TARE (TAR/2022/00072) and Council of Scientific and Industrial Research (Project No. 01(2934)/18/EMR-II), New Delhi, India.

ASSOCIATED CONTENT

Supporting Information

The Supporting Information is available free of charge at https://pubs.acs.org/doi/xxxx.

Supporting information for this article, Experimental procedures, optimized geometry, frontier orbitals, and additional transient spectral data.

Author Information

Corresponding Author

Prof. Rajneesh Misra – Department of Chemistry, Indian Institute of Technology, Indore-453552, India. E-mail: rajneeshmisra@iiti.ac.in

Prof. Francis D'Souza – Department of Chemistry, University of North Texas, 1155 Union Circle, #305070, Denton, TX 76203-5017, USA, E-mail: Francis.DSouza@UNT.edu

Authors

Dr. Youngwoo Jang – Department of Chemistry, University of North Texas, 1155 Union Circle, #305070, Denton, TX 76203-5017, USA

Dr. Bijesh Sekaran – Department of Chemistry, Indian Institute of Technology, Indore-453552, India.

Prabal P. Singh - Department of Chemistry, Indian Institute of Technology, Indore-453552, India.

Conflict of Interest

There are no conflicts to declare.

References and Notes

- (1) Torres, T.; Bottari, G. Organic Nanomaterials: Synthesis, Characterization, and Device Applications. Eds: T. Torres and G. Bottari, John Wiley & Sons, Inc., Hoboken, NJ, 2013.
- (2) Imahori, H.; Umeyama, T.; Ito, S. Large π -Aromatic Molecules as Potential Sensitizers for Highly Efficient Dye-Sensitized Solar Cells. *Acc. Chem. Res.* **2009**, *42* (11), 1809–1818.
- (3) Gust, D.; Moore, T. A.; Moore, A. L. Realizing Artificial Photosynthesis. *Faraday Discuss* **2012**, *155*, 9–26.
- (4) Bottari, G.; de la Torre, G.; Guldi, D. M.; Torres, T. Covalent and Noncovalent Phthalocyanine–Carbon Nanostructure Systems: Synthesis, Photoinduced Electron Transfer, and Application to Molecular Photovoltaics. *Chem. Rev.* **2010**, *110* (11), 6768–6816.
- (5) Fukuzumi, S.; Ohkubo, K.; Suenobu, T. Long-Lived Charge Separation and Applications in Artificial Photosynthesis. *Acc. Chem. Res.* **2014**, *47* (5), 1455–1464.
- (6) Barrejón, M.; Arellano, L. M.; D'Souza, F.; Langa, F. Bidirectional Charge-Transfer Behavior in Carbon-Based Hybrid Nanomaterials. *Nanoscale* **2019**, *11* (32), 14978–14992.

- (7) KC, C. B.; D'Souza, F. Design and Photochemical Study of Supramolecular Donor–Acceptor Systems Assembled via Metal–Ligand Axial Coordination. Coord. *Chem. Rev.* **2016**, *322*, 104–141.
- (8) Schmitz, C.; Pösch, P.; Thelakkat, M.; Schmidt, H.-W.; Montali, A.; Feldman, K.; Smith, P.; Weder, C. Polymeric Light-Emitting Diodes Based on Poly(p-Phenylene Ethynylene), Poly(Triphenyldiamine), and Spiroquinoxaline. *Adv. Funct. Mater.* **2001**, *11* (1), 41–46.
- (9) Chung, W.-S.; Liu, J.-H. Quinoxalino-Fused Sultines and Their Application in Diels–Alder Reactions. *Chem. Commun.* **1997**, *2*, 205–206.
- (10) Boxi, S.; Jana, D.; Ghorai, B. K. Synthesis and Optical Properties of Bipolar Quinoxaline-Triphenylamine Based Stilbene Compounds. *Opt. Mater. X* **2019**, *I*, 100013.
- (11) Czerwieniec, R.; Herbich, J.; Kapturkiewicz, A.; Nowacki, J. Radiative Electron Transfer in Planar Donor–Acceptor Quinoxaline Derivatives. *Chem. Phys. Lett.* **2000**, *325* (5–6), 589–598.
- (12) Cao, X.; Jin, F.; Li, Y.-F.; Chen, W.-Q.; Duan, X.-M.; Yang, L.-M. Triphenylamine-Modified Quinoxaline Derivatives as Two-Photon Photoinitiators. *New J. Chem.* **2009**, *33* (7), 1578.
- (13) Ishi-I, T.; Ikeda, K.; Kichise, Y.; Ogawa, M. Red-Light-Emitting System Based on Aggregation of Donor–Acceptor Derivatives in Polar Aqueous Media. *Chem. Asian J.* **2012**, 7, 1553-1558.
- (14) Lu, X.; Fan, S.; Wu, J.; Jia, X.; Wang, Z.-S.; Zhou, G. Controlling the Charge Transfer in D–A–D Chromophores Based on Pyrazine Derivatives. *J. Org. Chem.* **2014**, *79*, 6480-6489.
- (15) Wen, Z.; Yang, T.; Zhang, D.; Wang, Z.; Dong, S.; Xu, H.; Miao, Y.; Zhao, B.; Wang, H. A Multifunctional Luminescent Material Based on Quinoxaline and Triphenylamine Groups: Polymorphism, Mechanochromic Luminescence, and Applications in High-Efficiency Fluorescent OLEDs. *J. Mater. Chem. C* **2022**, *10*, 3396-3403.
- (16) Thomas, J.; K. R.; Lin, J. T.; Tao, Y.-T.; Chuen, C.-H. Quinoxalines Incorporating Triarylamines: Potential Electroluminescent Materials with Tunable Emission Characteristics. *Chem. Mater.* **2002**, *14* (6), 2796–2802.
- (17) Huang, T.-H.; Whang, W.-T.; Shen, J. Y.; Wen, Y.-S.; Lin, J. T.; Ke, T.-H.; Chen, L.-Y.; Wu, C.-C. Dibenzothiophene/Oxide and Quinoxaline/Pyrazine Derivatives Serving as Electron-Transport Materials. *Adv. Funct. Mater.* **2006**, *16* (11), 1449–1456.

- (18) Wang, X.; Zhou, Y.; Lei, T.; Hu, N.; Chen, E.-Q.; Pei, J. Structural-Property Relationship in Pyrazino[2,3-g] Quinoxaline Derivatives: Morphology, Photophysical, and Waveguide Properties. *Chem. Mater.* **2010**, *22* (12), 3735–3745.
- (19) Thomas, J.; K. R.; Velusamy, M.; Lin, J. T.; Chuen, C.-H.; Tao, Y.-T. Chromophore-Labeled Quinoxaline Derivatives as Efficient Electroluminescent Materials. *Chem. Mater.* **2005**, *17* (7), 1860–1866.
- (20) Dailey, S.; Feast, W. J.; Peace, R. J.; Sage, I. C.; Till, S.; Wood, E. L. Synthesis and Device Characterisation of Side-Chain Polymer Electron Transport Materials for Organic Semiconductor Applications. *J. Mater. Chem.* **2001**, *11* (9), 2238–2243.
- (21) Gupta, S.; Milton, M. D. Novel Y-Shaped AIEE-TICT Active π-Extended Quinoxalines-Based Donor–Acceptor Molecules Displaying Acidofluorochromism and Temperature Dependent Emission. *J. Photochem. Photobiol. Chem.* **2022**, *424*, 113630.
- (22) Sekita, M.; Ballesteros, B.; Diederich, F.; Guldi, D. M.; Bottari, G.; Torres, T. Intense Ground-State Charge-Transfer Interactions in Low-Bandgap, Panchromatic Phthalocyanine—Tetracyanobuta-1,3-Diene Conjugates. *Chem. Int. Ed.* **2016**, *55* (18), 5560–5564.
- (23) Winterfeld, K. A.; Lavarda, G.; Guilleme, J.; Sekita, M.; Guldi, D. M.; Torres, T.; Bottari, G. Subphthalocyanines Axially Substituted with a Tetracyanobuta-1,3-Diene–Aniline Moiety: Synthesis, Structure, and Physicochemical Properties. *J. Am. Chem. Soc.* **2017**, *139* (15), 5520–5529.
- (24) Winterfeld, K. A.; Lavarda, G.; Guilleme, J.; Guldi, D. M.; Torres, T.; Bottari, G. Subphthalocyanine–Tetracyanobuta-1,3-Diene–Aniline Conjugates: Stereoisomerism and Photophysical Properties. *Chem. Sci.* **2019**, *10* (48), 10997–11005.
- (25) Gautam, P.; Misra, R.; Thomas, M. B.; D'Souza, F. Ultrafast Charge-Separation in Triphenylamine-BODIPY-Derived Triads Carrying Centrally Positioned, Highly Electron-Deficient, Dicyanoquinodimethane or Tetracyanobutadiene Electron-Acceptors. *Chem. Eur. J.* **2017**, *23* (38), 9192–9200.
- (26) Sharma, R.; Thomas, M. B.; Misra, R.; D'Souza, F. Strong Ground- and Excited-State Charge Transfer in C 3 -Symmetric Truxene-Derived Phenothiazine-Tetracyanobutadine and Expanded Conjugates. *Angew. Chem. Int. Ed.* **2019**, *131* (13), 4394–4399.
- (27) Poddar, M.; Jang, Y.; Misra, R.; D'Souza, F. Excited-State Electron Transfer in 1,1,4,4-Tetracyanobuta-1,3-Diene (TCBD)- and Cyclohexa-2,5-Diene-1,4-Diylidene-Expanded TCBD-Substituted BODIPY-Phenothiazine Donor–Acceptor Conjugates. *Chem. Eur. J.* **2020**, *26* (30), 6869–6878.

- (28) Khan, F.; Jang, Y.; Patil, Y.; Misra, R.; D'Souza, F. Photoinduced Charge Separation Prompted Intervalence Charge Transfer in a Bis(Thienyl)Diketopyrrolopyrrole Bridged Donor-TCBD Push-Pull System. *Angew. Chem. Int. Ed.* **2021**, *133* (37), 20681–20690.
- (29) Yadav, I. S.; Alsaleh, A. Z.; Misra, R.; D'Souza, F. Charge Stabilization via Electron Exchange: Excited Charge Separation in Symmetric, Central Triphenylamine Derived, Dimethylaminophenyl–Tetracyanobutadiene Donor–Acceptor Conjugates. *Chem. Sci.* **2021**, *12* (3), 1109–1120.
- (30) Kivala, M.; Boudon, C.; Gisselbrecht, J. -P.; Seiler, P.; Gross, M.; Diederich, F. Charge-Transfer Chromophores by Cycloaddition–Retro-Electrocyclization: Multivalent Systems and Cascade Reactions. *Angew. Chem. Int. Ed.* **2007**, *46*, 6357-6360.
- (31) Michinobu, T.; Boudon, I.; Gisselbrecht, J. -P; Seiler, P.; Frank, B.; Moonen, N. N. P.; Gross, M.; Diederich, F. Donor-Substituted 1,1,4,4-Tetracyanobutadienes (TCBDs): New Chromophores with Efficient Intramolecular Charge-Transfer Interactions by Atom-Economic Synthesis. *Chem. Eur. J.* **2006**, *12*, 1889-1905.
- (32) Shoji, T.; Ito, S.; Toyota, K.; Iwamoto, T.; Yasunami, M.; Morita, N. Reactions Between 1-Ethynylazulenes and 7,7,8,8-Tetracyanoquinodimethane (TCNQ): Preparation, Properties, and Redox Behavior of Novel Azulene-Substituted Redox-Active Chromophores. *Eur. J. Org. Chem.* **2009**, 4316-4324.
- (33) Bui, A. T.; Philippe, C.; Beau, M.; Richy, N.; Cordier, M.; Roisnel, T.; Lemiegre, L.; Mongin, O.; Paul, F.; Trolez, Y. Synthesis, Characterization and Unusual Near-Infrared Luminescence of 1,1,4,4-Tetracyanobutadiene Derivatives. *Chem. Commun.* **2020**, *56*, 3571-3574.
- (34) Yamada, M.; Schweizer, W. B.; Schoenebeck, F.; Diederich, F. Unprecedented Thermal Rearrangement of Push–Pull-Chromophore–[60]Fullerene Conjugates: Formation of Chiral 1,2,9,12-Tetrakis-Adducts. *Chem. Commun.* **2010**, *46*, 5334-5336.
- (35) Yamada, M.; Rivera-Fuentes, P.; Schweizer, W. B.; Diederich, F. Optical Stability of Axially Chiral Push-Pull-Substituted Buta-1,3-Dienes: Effect of a Single Methyl Group on the C₆₀ Surface. *Angew. Chem. Int. Ed.* **2010**, *49*, 3532-3535.
- (36) Rout, Y.; Jang, Y.; Gobeze, H. B.; Misra, R.; D'Souza, F. Conversion of Large-Bandgap Triphenylamine–Benzothiadiazole to Low-Bandgap, Wide-Band Capturing Donor–Acceptor Systems by Tetracyanobutadiene and/or Dicyanoquinodimethane Insertion for Ultrafast Charge Separation. *J. Phys. Chem. C* **2019**, *123*, 23382-23389.
- (37) Poddar, M.; Jang, Y.; Misra, R.; D'Souza, F. Excited-State Electron Transfer in 1,1,4,4-Tetracyanobuta-1,3-Diene (TCBD)- and Cyclohexa-2,5-Diene-1,4-Diylidene-

- Expanded TCBD-Substituted BODIPY-Phenothiazine Donor-Acceptor Conjugates. *Chem. Eur. J.* **2020**, *26*, 6869–6879.
- (38) Pinjari, D.; Alsaleh, A. Z.; Patil, Y.; Misra, R.; D'Souza, F. Interfacing High-Energy Charge-Transfer States to a Near-IR Sensitizer for Efficient Electron Transfer upon Near-IR Irradiation. *Angew. Chem. Int. Ed.* **2020**, *59*, 23697-23705.
- (39) Yadav, I. S.; Alsaleh, A. Z.; Misra, R.; D'Souza, F. Charge Stabilization *via* Electron Exchange: Excited Charge Separation in Symmetric, Central Triphenylamine Derived, Dimethylaminophenyl–Tetracyanobutadiene Donor–Acceptor Conjugates. *Chem. Sci.*, **2021**, *12*, 1109-1120.
- (40) Jang, Y.; Rout, Y.; Misra, R.; D'Souza, F. Symmetric and Asymmetric Push–Pull Conjugates: Significance of Pull Group Strength on Charge Transfer and Separation. *J. Phys. Chem. B.* **2021**, *125*, 4067-4075.
- (41) Shinde, J.; Thomas, M. B.; Poddar, M.; Misra, R.; D'Souza, F. Does location of BF₂-Chelated Dipyrromethene (BODIPY) Ring Functionalization Affect Spectral and Electron Transfer Properties? Studies on α-, β-, and meso-Functionalized BODIPY-Derived Donor–Acceptor Dyads and Triads. *J. Phys. Chem. C* **2021**, *125*, 23911-23921.
- (42) Yadav, I. S.; Jang, Y.; Rout, Y.; Thomas, M. B.; Misra, R.; D'Souza, F. Near-IR Intramolecular Charge Transfer in Strongly Interacting Diphenothiazene-TCBD and Diphenothiazene-TCNQ Push-Pull Triads. *Chem. Eur. J.* **2022**, e202200348.
- (43) Bureš, F.; Schweizer, W. B.; May, J. C.; Boudon, C.; Gisselbrecht, J.-P.; Gross, M.; Biaggio, I.; Diederich, F. Property Tuning in Charge-Transfer Chromophores by Systematic Modulation of the Spacer Between Donor and Acceptor. *Chem. Eur. J.* **2007**, *13* (19), 5378–5387.
- (44) Bijesh, S.; Misra, R. Triphenylamine Functionalized Unsymmetrical Quinoxalines. *Asian J. Org. Chem.* **2018**, *7* (9), 1882–1892.
- (45) Wu, J.; Zhang, L.; Ling, J.; Zeng, Q.; Yin B.; Li, X., Synthesis and Fluorescent Properties of Quinoxaline Derived Ionic Liquids. *Green Energy & Environment*, **2022**, 7, 996-1005.
- (46) Frisch, M. J.; Trucks, G. W.; Schlegel, H. B.; Scuseria, G. E.; Robb, M. A.; Cheeseman, J. R.; Scalmani, G.; Barone, V.; Mennucci, B.; Petersson, G. A., et. al. *Gaussian* 09, Revision A.1; Gaussian Inc.: Wallingford, CT, 2009.
- (47) Rehm, D.; Weller, A. Kinetics of Fluorescence Quenching by Electron and H-Atom Transfer. *Isr. J. Chem.* **1970**, *8* (2), 259–271.

(48) Gibbs free-energy change associated with excited-state charge separation (CS) and dark charge recombination (CR) were estimated according to equations i-iii

$$-\Delta G_{CR} = E_{ox} - E_{red} + \Delta G_{S} \qquad (i)$$

$$-\Delta G_{CS} = \Delta E_{00} - (-\Delta G_{CR})$$
 (ii)

where ΔE_{00} corresponds to the singlet state energy of 1. The term ΔG_S refers to electrostatic energy calculated according to the dielectric continuum model (see equation iii). The E_{ox} and E_{red} represent the oxidation potential and the first reduction potential, respectively.

$$\Delta G_{\rm S} = e^2/4 \pi \, \varepsilon_{\rm o} \left[-1/R_{\rm cc} \, \varepsilon_{\rm R} \right) \tag{iii}$$

The symbols ε_0 and ε_R represent the vacuum permittivity and dielectric constant of benzonitrile used for photochemical and electrochemical studies. R_{CC} is the center-to-center distance between donor and acceptor entities from the computed structures.

(49) Snellenburg, J. J., Laptenok, S., Seger, R., Mullen, K. M., & van Stokkum, I. H. Glotaran: A Java-Based Graphical User Interface for the R Package TIMP. *J. Stat. Softw.*, **2012**, 49, 1-22.

TOC Content

